Low-temperature spectral dynamics of excitons in molecular aggregates

Bednarz, M.; Malyshev, V.A.; Knoester, J.

Published in:
Journal of Luminescence

DOI:
10.1016/j.jlumin.2004.09.037

Publication date:
2005

Available online at www.sciencedirect.com
SCIENCE DIRECT®
Journal of Luminescence 112 (2005) 411–415
JOURNAL OF LUMINESCENCE
www.elsevier.com/locate/jlumin

Low-temperature spectral dynamics of excitons in molecular aggregates

M. Bednarz[a,b,*], V.A. Malyshev[b,1], J. Knoester[b]

[a] *Abteilung Theoretische Physik, Universität Ulm, Albert-Einstein-Allee 11, 89069 Ulm, Germany*
[b] *Institute for Theoretical Physics and Material Science Center, University of Groningen, Nijenborgh 4, 9747 AG Groningen, The Netherlands*

Available online 24 December 2004

Abstract

Fluorescence spectra under various excitation and detection conditions are put forward to probe exciton spectral dynamics, resulting from hopping of excitons over localized states. We address the complexity of the exciton spectral dynamics, which is a direct consequence of the interplay of localization, intra-band relaxation and radiative relaxation of excitons.

PACS: 71.23.An; 71.35.Cc

Keywords: Static disorder; Frenkel excitons; Exciton transport

1. Introduction

Over the past 15 years, much theoretical and experimental effort has been directed to understanding the transport and optical dynamics of Frenkel excitons in molecular aggregates. The reason is that aggregates exhibit extraordinary optical properties, which are promising from both the fundamental and practical point of view [1]. In particular, the fluorescence decay time in J-aggregates grows with increasing temperature [2], reflecting the superradiant nature of Frenkel exciton states coupled to the light. Some aggregates show a counter-intuitive non-monotonic temperature dependence of the Stokes shift of the fluorescence spectrum [3]. Femtosecond optical dynamics in squarylium dye J-aggregates was recently reported [4].

The goal of the present paper is to analyze theoretically the low-temperature spectral dynamics of excitons caused by the vibration-assisted hopping over localized states. Exciton fluorescence

*Corresponding author. Tel.: +49 731 50 22 909; fax: +49 731 50 22 924.
E-mail address: mariusz.bednarz@physik.uni-ulm.de (M. Bednarz).
[1] On leave from "S.I. Vavilov State Optical Institute", 199034 Saint-Petersburg, Russia.

0022-2313/$ - see front matter © 2004 Elsevier B.V. All rights reserved.
doi:10.1016/j.jlumin.2004.09.037

spectra under various excitation conditions are put forward to uncover the regularities of the exciton spectral dynamics. The Pauli master equation is used as a tool to describe exciton hopping. We show that the low-temperature relaxation of excitons is dominated by the local energy structure which has been proven to exists in the low-energy tail of the density of exciton states [5]. Thus, this structure can be monitored by means of fluorescence measurements.

2. Model

We model an aggregate as an open regular chain of N ($N \gg 1$) two-level molecules with parallel transition dipole moments. The optical excitations of the aggregate are Frenkel excitons which are described by the Hamiltonian $H_{\mathrm{ex}} = \sum_{n=1}^{N} \varepsilon_n |n\rangle\langle n| + \sum_{n,m}^{N} J_{nm} |n\rangle\langle m|$, were $|n\rangle$ is the state vector of a single excitation at the nth site with the energy ε_n. The on-site energies ε_n are assumed to be uncorrelated (for different sites) Gaussian stochastic variables with zero mean and standard deviation σ. The inter-site interactions J_{nm} ($J_{nn} \equiv 0$) are considered to be non-fluctuating and being of dipole–dipole origin: $J_{nm} = -J/|n-m|^3$ ($J_{nn} \equiv 0$). The nearest-neighbor coupling J is assumed to be positive (J-aggregates). Then, the optically dominant states are those at the bottom of the exciton band, and they are of our primary interest. Diagonalizing the Hamilton matrix $H_{nm} = \langle n|H|m\rangle$ yields the exciton eigenenergies E_ν ($\nu = 1, 2, \ldots, N$) and wave functions $\varphi_{\nu n}$, which we use as a basis in our further treatment. Because of the disorder-induced localization effect, the wave functions $\varphi_{\nu n}$ do not extend over the entire chain. They are localized on finite segments of typical size $N^* < N$. The wave functions of the bottom states of different segments overlap weakly, while those localized on the same segment form manifolds of a few states [5].

The coupling of excitons to host vibrations results in hopping of excitons from one localized state to the others. In order to describe the kinetics of hopping and radiative emission processes, we employ the master equation for the populations $P_\nu(t)$ of the localized exciton states [6]

$$\dot{P}_\nu = R_\nu - \gamma_\nu P_\nu + \sum_{\nu'=1}^{N} (W_{\nu\nu'} P_{\nu'} - W_{\nu'\nu} P_\nu), \tag{1}$$

where R_ν denotes the constant rate of optically creating populations in the νth exciton state by a pump pulse, $\gamma_\nu = \gamma_0 (\sum_{n=1}^{N} \varphi_{\nu n})^2$ is the spontaneous emission rate of the νth excitonic state, γ_0 being the spontaneous emission rate of a monomer. The hopping rate $W_{\nu\nu'}$ from the state ν' to ν is proportional to the overlap integral of the corresponding wave functions, $I_{\nu\nu'} = \sum_n \varphi_{\nu n}^2 \varphi_{\nu' n}^2$, and is given by [6]

$$W_{\nu\nu'} = S(|\varepsilon_{\nu\nu'}|) I_{\nu\nu'} \begin{cases} \Theta(\varepsilon_{\nu\nu'}) n(\varepsilon_{\nu\nu'}), \\ \Theta(-\varepsilon_{\nu\nu'})[n(-\varepsilon_{\nu\nu'}) + 1]. \end{cases} \tag{2}$$

Here, $\varepsilon_{\nu\nu'} = E_\nu - E_{\nu'}$, $n(\varepsilon_{\nu\nu'}) = [\exp(\varepsilon_{\nu\nu'}/k_{\mathrm{B}}T) - 1]^{-1}$ is the mean occupation number of a normal vibration mode with the energy $\varepsilon_{\nu\nu'}$, k_{B} is the Boltzmann constant, and $\Theta(x) = 1\,(0)$ if $x > 0$ ($x < 0$). The spectral function $S(\varepsilon_{\nu\nu'})$ depends on the model of the exciton–vibration interaction. We set hereafter $S(\varepsilon_{\nu\nu'}) = W_0 |E_\nu - E_{\nu'}|/J$ to account for the long-wavelength acoustic limit. The constant W_0 is a model dependent parameter that characterizes the overall strength of the phonon-assisted exciton scattering. It will be used in the following as a free parameter. The hopping rates given by Eq. (2) obey the principle of detailed balance, which guarantees that eventually the excitons arrive at the proper equilibrium state characterized by the Boltzmann distribution over energy.

3. Numerical results and discussions

3.1. Stokes shift

We first address the temperature dependence of the steady-state exciton fluorescence spectrum which is defined as $I(E) = (1/N)\langle \sum_\nu \delta(E - E_\nu) \gamma_\nu P_\nu^{\mathrm{st}} \rangle$ where P_ν^{st} is the steady-state solution of Eq. 1 (at $\dot{P}_\nu = 0$). We focus on the Stokes shift of the fluorescence spectrum with respect to the absorption band. Figure 1 (upper panel) shows the results obtained under the conditions of a

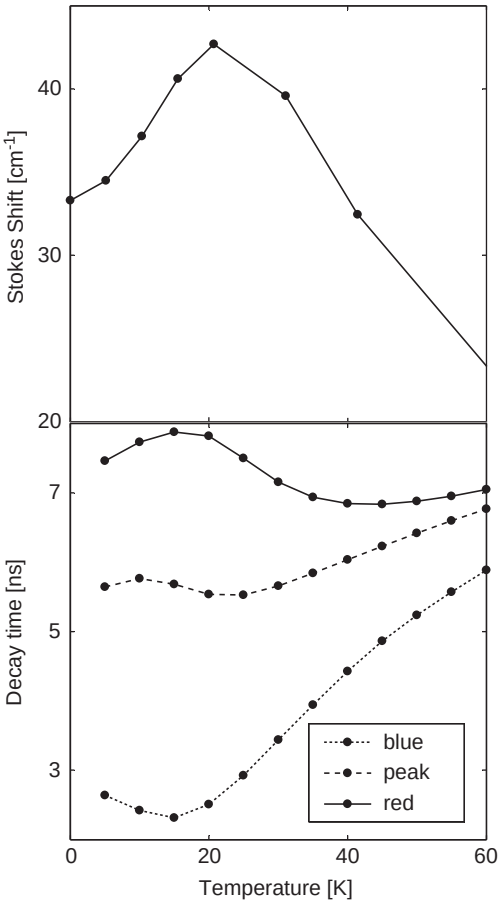

Fig. 1. Temperature dependence of the Stokes shift (upper panel) and of the decay time of the exciton fluorescence. The three curves in the lower panel correspond to different detection energies E_d related to the steady-state fluorescence spectrum at 10 K as a reference: detection at half-maximum on the red side of the fluorescence peak (solid line), at the fluorescence maximum (dashed line), and at a half-maximum on the blue side (dotted line). The parameters used in the simulations are $N = 500$, $J = 740\,\mathrm{cm}^{-1}$, $\gamma_0 = 2.7 \times 10^{-7}\,\mathrm{J}$, $\sigma = 0.23\,\mathrm{J}$, $W_0 = 30\,\mathrm{J}$. Dots mark the numerical data, while the lines connecting the dots are guides to the eye.

narrow energy window excitation in the blue-tail of the absorption band for the parameters $J = 740\,\mathrm{cm}^{-1}$, $\gamma_0 = 2.7 \times 10^{-7}\,\mathrm{J}$, $\sigma = 0.23\,\mathrm{J}$, and $W_0 = 30\,\mathrm{J}$, which are characteristic for aggregates of 3, 3′-bis(sulfopropyl)-5, 5′-dichloro-9-ethylthiacarbocyanine (THIATS) [3,6]. We observe from Fig. 1 that a counter-intuitive non-monotonous behavior of the Stokes shift occurs in the range 0–20 K. This is a clear indication that excitons are not thermalized below 20 K, otherwise the Stokes shift should decrease upon increasing the temperature. At these temperatures, thermalization within the time scale of radiative emission is impossible. For the lower exciton states, $W_{vv'} < \gamma_v$ due to the weak overlap of the wave functions, and hopping, which tends to equilibrate the excitonic system, is interrupted. As a result, the lowest states turn out to be unavailable for excitons at zero temperature. They, however, can be populated upon increasing the temperature via higher lying band states, which are delocalized over several localization segments [6]. This indirect hopping is responsible for an increase of the Stokes shift at small temperatures compared to the absorption bandwidth. Further heating thermalizes the excitons and results in a decrease of the Stokes shift. This nonmonotonic behavior was observed in experiments on THIATS dye aggregates [3].

3.2. Decay time

Now we address the temperature dependence of the fluorescence decay time τ at different detection energies E_d, analyzing the fluorescence kinetics, $I(E_d; t) = \langle \sum_v \gamma_v P_v(t) \Delta(E_d - E_v) \rangle$. The window function $\Delta(E_d - E_v)$ is unity for $|E_d - E_v| < 0.0025\,\mathrm{J}$ and zero otherwise. We considered deep-blue-tail short-pulse excitation conditions and calculated τ for three detection energies: at the peak position and at half-maximum of the red and blue sides of the steady-state fluorescence spectrum at 10 K. In other words, we try to focus on the decay of different states with different localization lengths. From the intensity traces, we extracted the fluorescence decay time $\tau_e(E_d)$ as the time it takes the fluorescence intensity $I(E_d, t)$ to decay to $1/e$ of its peak value. The results as a function of temperature are shown in lower panel of Fig. 1.

At zero temperature the decay times clearly differ for the three detection energies. For the red-side detection, we observe a longer decay time as compared to the case of the peak- and blue-side detection. This indicates that at the red side the decay time at zero temperature is determined completely by radiative decay; hopping has no

effect on this energy because of the low probability of occurrence of neighboring segments with low energy. For the detection at the peak and blue position, we find a zero-temperature decay time which is faster than the purely radiative time. The difference is due to relaxation to lower lying exciton states in neighboring segments. At high temperature the decay times for the different detection energies approach each other. This is a consequence of the fact that the scattering rates are then large enough for the exciton populations to become equilibrated on the time scale of emission.

The key observation is that the temperature dependence is non-monotonic within the same temperature range for which the Stokes shift behaves non-monotonically (cf. Fig. 1, upper panel). We attribute this behavior to the same temperature activated inter-segment relaxation via higher lying exciton states. At the blue detection side (which still lies in the tail of the density of states), this effect leads to a decrease in the lifetime, as it opens extra decay channels. On the red side, the situation is more subtle. This energy is so deep in the red tail of the density of states, that even the activated migration hardly opens new channels for decay. In fact, the activated relaxation occurring at the blue side toward lower energies will lead to extra contributions to the fluorescence intensity at the red side and, thus, to a growth of the decay time at this energy. At the peak position, we deal with the intermediate situation.

3.3. Resonant selective excitation

We also performed simulations of steady-state fluorescence spectra at 0 K, exciting fluorescence resonantly within a very narrow window in order to study down-hill relaxation only but with high precision. The results are shown in Fig. 2. As is seen, the fluorescence spectra are composed of a narrow peak at the excitation energy and a red-shifted wing. This spectral structure has a simple explanation within the framework of the band-edge local level structure. The narrow peak results from the localized exciton states (mostly with large oscillator strength) created by the pump, while the wing is formed due to possible hopping of initially

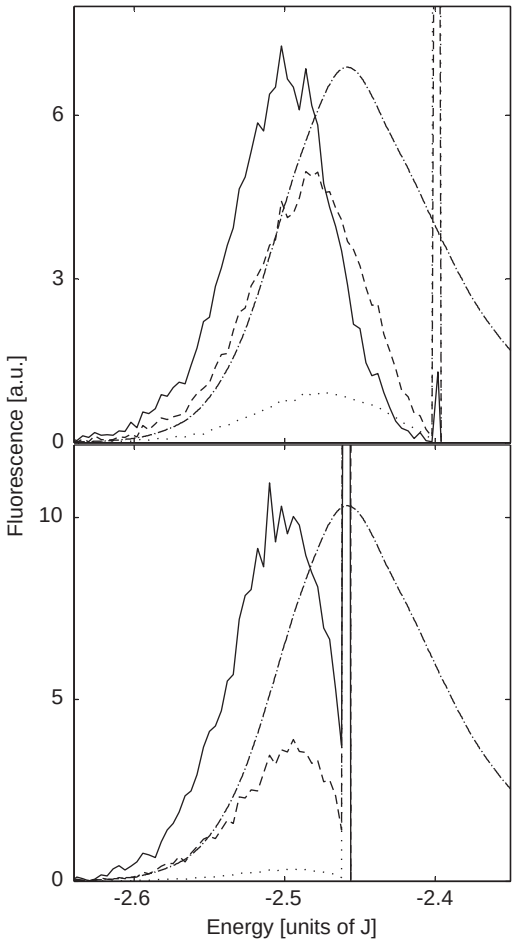

Fig. 2. Zero-temperature exciton fluorescence spectra calculated after selective excitation within a narrow window of width 0.001 J for different scattering rates: $W_0 = 0.001$ J (dotted lines), $W_0 = 0.1$ J (dashed lines), $W_0 = 30$ J (solid lines). The dash-dotted curve shows the absorption spectrum. Panels, upper and bottom, represent spectra obtained under the condition of excitation in the blue wing of the absorption spectrum and at its peak, respectively. Forty-thousand disorder realizations were considered. Other parameters are the same as in Fig. 1.

created excitons to the lower energy localized states, occurring within the same localization segment as well as between different ones.

We see that under excitation at the blue side of the absorption band, the fluorescence spectra are very sensitive to the value of W_0 (see Fig. 2, upper panel); one observes changes in both the amplitude and the Stokes shift of the red wing. The latter

indicates that the inter-segment hops are important in forming the wing. Bottom panel of Fig. 2 represents the results of simulations under excitation at the maximum of the absorption band. Here, the red wing exhibits changes in its amplitude upon changing W_0 only; the Stokes shift remains unchanged. This can be easily demonstrated by rescaling the red wings from the bottom panel of Fig. 2 to the same amplitude. We thus conjecture that under excitation at the maximum of the absorption band the red wing is dominated by the relaxation to the deep tail states of the density of states, independently of whether the relaxation is fast or slow. This provides us with a tool to study these states by fluorescence line narrowing spectroscopy. Details will be published elsewhere.

4. Summary and concluding remarks

In this paper, we theoretically studied the spectral dynamics in a one-dimensional Frenkel exciton system. On the basis of our numerical simulations, we conclude that the complexity of the exciton spectral dynamics results from interplay of localization, intra-band relaxation and radiative emission. We suggest fluorescence line narrowing measurements as an experimental tool to study intra-segment exciton relaxation.

Acknowledgements

M.B. gratefully acknowledges Deutsche Forschungsgemeinschaft for financial support within a SFB 569 grant.

References

[1] J. Knoester, Organic Nanostructures: Science and Application, IOS Press, Amsterdam, 2002, pp. 149–186.
[2] H. Fidder, J. Knoester, D.A. Wiersma, Chem. Phys. Lett. 171 (1990) 529;
H. Fidder, J. Terpstra, D.A. Wiersma, J. Chem. Phys. 94 (1991) 6895.
[3] I.G. Scheblykin, M.M. Bataiev, M. Van der Auweraer, A.G. Vitukhnovsky, Chem. Phys. Lett. 316 (2000) 37;
I.G. Scheblykin, O.Yu. Sliusarenko, L.S. Lepnev, A.G. Vitukhnovsky, M. Van der Auweraer, J. Phys. Chem. B 105 (2001) 4636.
[4] M. Furuki, M. Tian, Y. Sato, L.S. Pu, Appl. Phys. Lett. 78 (2001) 2634;
M. Furuki, M. Tian, Y. Sato, L.S. Pu, J. Lumin. 94–95 (2001) 369.
[5] A.V. Malyshev, V.A. Malyshev, Phys. Rev. B 63 (2001) 195111;
A.V. Malyshev, V.A. Malyshev, J. Lumin. 94–95 (2001) 369.
[6] M. Bednarz, V.A. Malyshev, J. Knoester, Phys. Rev. Lett. 91 (2003) 217401;
M. Bednarz, V.A. Malyshev, J. Knoester, J. Chem. Phys. 120 (2004) 3827.